Power-Spectrum-Based Wavelet Transform for Nonintrusive Demand Monitoring and Load Identification

Hsueh-Hsien Chang, *Member, IEEE*, Kuo-Lung Lian, *Member, IEEE*, Yi-Ching Su, and Wei-Jen Lee, *Fellow, IEEE*

***Abstract*—Though the wavelet transform coefficients (WTCs) contain plenty of information needed for turn-on/off transient signal identification of load events, adopting the WTCs directly requires longer computation time and larger memory requirements for the nonintrusive load monitoring identification process. To effectively reduce the number of WTCs representing load turn-on/off transient signals without degrading performance, a power spectrum of the WTCs in different scales calculated by Parseval's theorem is proposed and presented in this paper. The back-propagation classification system is then used for artificial neural network construction and load identification. The high success rates of load event recognition from both experiments and simulations have proved that the proposed algorithm is applicable in multiple load operations of nonintrusive demand monitoring applications.**

***Index Terms*—Artificial neural networks (ANNs), load identification, nonintrusive load monitoring (NILM), Parseval's theorem, wavelet transform (WT).**

I. Introduction

THE idea of nonintrusive load monitoring (NILM) was first developed in the 1980s at MIT by Hart [1]. NILM refers to a method of detecting the current energy consumptions of a house or a building using a single set of sensors at the electrical service entry (ESE) [2]. Fig. 1 shows a typical NILM system. Single-phase two-wire and single-phase three-wire systems are generally used to run a typical residential or an office building system. As shown in the figure, the secondary side of the ESE transformer, the voltage and the current at ESE are measured and sent to the meter database management system. These data are processed by the NILM algorithm to identify the operation statuses and energy/power consumption for individual or composite loads.

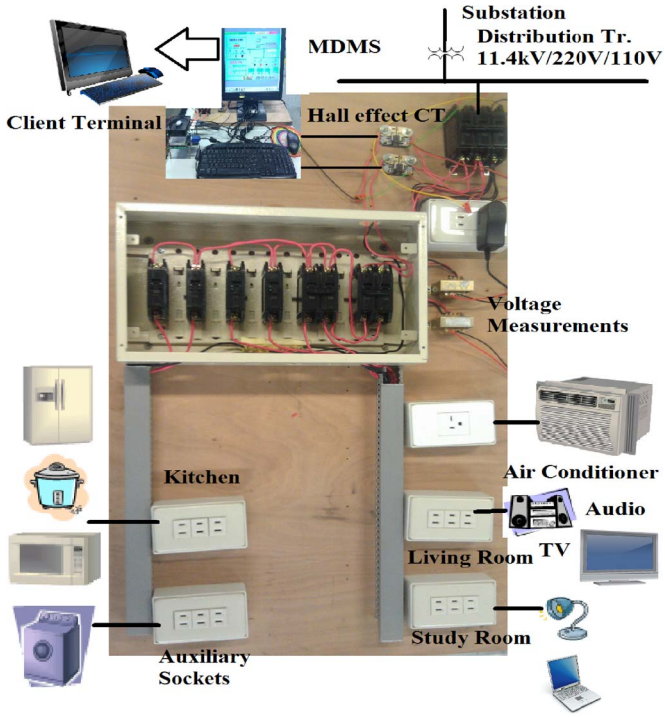

Fig. 1. Load identification system for an NILM system.

The NILM, in contrast with the traditional supervisory control and data acquisition (SCADA)-based system, can drastically reduce hardware and maintenance costs because only one set of voltage and current sensors is needed at ESE [1]. To have the same or comparable level of detection accuracy with the SCADA-based system, the NILM algorithm needs to be smart enough to disaggregate the loads based on their "power signatures" (PS) [2]. Over the past two decades, there have been many methods proposed for establishing various PS and identification methods for the NILM. References [3] and [4] provide a comprehensive review of the literature. The most frequently cited methods and recent related publications are briefly discussed in this paper. Hart used the variations of real, i.e., P, and reactive, i.e., Q, powers to detect the status of loads in the $P-Q$ plane [2]. However, the voltage variations of the utility may result in overlapping of loads in the $P-Q$ plane [5], different loads may consume the same real and reactive powers, and appliances that have nondiscrete changes in power

Manuscript received May 21, 2013; revised August 5, 2013 and September 16, 2013; accepted September 17, 2013. Date of publication September 24, 2013; date of current version May 15, 2014. Paper 2013-ESC-224.R2, presented at the 2013 Industry Applications Society Annual Meeting, Orlando, FL, USA, October 6–11, and approved for publication in the IEEE TRANSACTIONS ON INDUSTRY APPLICATIONS by the Energy Systems Committee of the IEEE Industry Applications Society. This work was supported by the National Science Council of Taiwan under Contract NSC 102-2221-E-228-002.

H.-H. Chang is with JinWen University of Science and Technology, New Taipei 23154, Taiwan (e-mail: sschang@just.edu.tw).

K.-L. Lian is with National Taiwan University of Science and Technology, Taipei 106, Taiwan (e-mail: ryankuolian@gmail.com).

Y.-C. Su is with Chicony Electronics Company, Ltd., New Taipei 24891, Taiwan (e-mail: hello0716@hotmail.com).

W.-J. Lee is with the Energy Systems Research Center and the Department of Electrical Engineering, The University of Texas at Arlington, Arlington, TX 76019 USA (e-mail: wlee@uta.edu).

Color versions of one or more of the figures in this paper are available online at http://ieeexplore.ieee.org.

Digital Object Identifier 10.1109/TIA.2013.2283318

consumption may not be identified [6]. Akbar and Khan [5] have proposed the use of current harmonics as the PS. However, it will be difficult to apply this method for linear or quasi-linear loads since their harmonic contents are very low. In addition to the steady-state power draw, Albicki and Cole [7] have proposed to use edges and slopes as appliance features. However, this method is only suitable for appliances with significant spikes in power draw [3]. Leeb *et al.* have used the "spectral envelope" (SE) concept [8] for a NILM system. The SE is a vector of the first several coefficients of the short-time Fourier transform (STFT) of the transient current signal. Although this method can detect numerous appliances, including the variable loads, it requires extensive training for each appliance before classification and monitoring can be performed. Patel *et al.* have proposed to monitor electric noise on the power line caused by the switching of electrical loads in a socket for transient signal [9]. In this paper, the authors assumed that the noise signature of a particular electrical load depends both on the load and the transmission line behavior of the interconnecting power line. However, as suggested in [10], the appliance signature may depend on the household electrical wiring so that an appliance connected to a different socket may not be correctly detected. Lam *et al.* [11] have proposed to employ I–V curves for characterizing different loads. Nevertheless, such an algorithm has not yet been successfully applied to a NILM system. Yang *et al.* [12] employed a turn-on transient energy algorithm for load identifications. However, this algorithm requires a high sampling rate to accurately capture the detailed variations in the transient energy. For the load identification methods, the optimization methods' objectives are usually to minimize the residue between the PS of the unknown loads with those from the known database. However, the problem becomes complex when the unknown is a composite load. In [4], the authors have proposed combining several of the existing algorithms such as the real and reactive power $(P-Q)$ method, the eigenvalue method, and the instantaneous power waveform to form the committee decision mechanism. However, the problem of this method is that identification of a load will lead to indecisive results if a tie is reached by the committee. Recently, there has been a growing interest in improving the performance of recognition by using artificial intelligence methods such as artificial neural network (ANN). Srinivasan *et al.* [13] proposed a neural network (NN)-based approach to identify harmonic sources. However, the method does not incorporate the various operation modes for each load. In [14], the authors have also applied particle swarm optimization to optimize the parameters of training algorithms in NN. Nevertheless, the resulting training time could be quite long. In an effort to overcome some of the aforementioned problems, a new NILM system, which employs a wavelet multiresolution analysis (WMRA) technique, Parseval's theorem, and a back-propagation ANN (BP-ANN), is proposed in this paper.

Many researchers proposed some applications in specific loads or appliances to estimate load identification for NILM systems. Lee *et al.* [15] proposed a variable-speed-drive power estimation method to track nonintrusively variable-demand loads. He *et al.* [16] analyzed front-end power supply circuit topologies and extracted features that can uniquely distinguish the individual miscellaneous electric loads (MELs) types by using the model-driven hierarchical feature extraction.

Depending upon the applications, there are various ways of collecting/sampling the ESE signals. A simple meter with a low frequency is cheap but can only provide P and Q measurements. On the other hand, a multifunction meter with high-frequency data acquisition (DAQ) is more expensive but can provide transient signals, harmonics, P and Q measurement, etc. The DAQ module that Hart used was the former one. Since the power signature was based on P and Q, the on/off event is mainly for the major appliances. Since the cost of a multifunction DAQ module is much lower compared with that in the 1980s, it becomes feasible to perform both the major loads and MELs for load identification.

The proposed algorithms of this paper may have difficulty in handling similar loads with similar transient waveforms. In such a case, additional information is needed for identification [17].

The discrete wavelet transform (DWT) technology has been often used to capture the time of transient occurrence [18]. Integrating the DWT technology with the artificial intelligence method or expert system becomes a promising approach for a nonintrusive event classifier to improve the load events recognition of an NILM system. However, the following issues must be overcome before their practicality can be realized [19].

1) Directly adopting the DWT coefficients as inputs to the NNs requires large memory space and long training time.
2) The decomposition level with the number of extraction features must be reduced to enhance computation efficiency and improve the accuracy of load event recognition of the NILM system.

This paper presents a novel classifier consisting of two models, as shown in Fig. 2. First, the WMRA technique and Parseval's theorem are utilized to extract the energy distribution features of the individual event turn-on/off transient signal at different resolution levels. Second, the BP-ANN is employed to classify load types according to the detailed energy distribution. By using Parseval's theorem, the number of transient signal features can be reduced without losing its fidelity.

This paper proposes useful feature extraction techniques that are applicable in multiple load operations of nonintrusive demand monitoring applications to distinguish the types or classes within a predetermined load set.

The accuracy rate and the computation requirement of the proposed method were tested in a model system and simulated by using Electromagnetic Transient Program (EMTP) software. These results showed that the proposed method can analyze the signals efficiently and effectively, thus enhancing the performance of the demand monitoring and load identification in the NILM system.

II. Proposed Load Identification System

The block diagram in Fig. 2 includes the algorithms of turn-on/off transient event detection (TOOTED), the processes of the WT technique, extracting the features from transient signals, and the BP-ANN classification network. The procedures of recognizing load signals belonging to certain kinds of the load

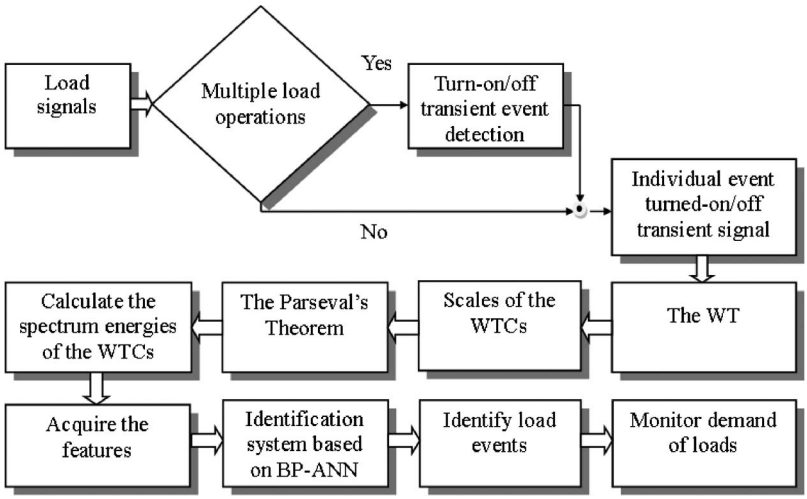

Fig. 2. Block diagram of a load event identification system.

events are described as follows. First, load operation modes are distinguished (i.e., individual or multiple load operations). A turn-on/off time of transient event after steady-state loads is detected by the algorithm of TOOTED when multiple load operations occur. Then, an individual event turned-on/off transient signal can be acquired by removing the steady-state current signals before the occurrence of the event [20].

A current waveform of the individual event turned-on/off transient signal is transferred using wavelet transform (WT) to obtain the different scales of the WT coefficients (WTCs). Although all scales of the WTCs of the load turned-on/off transient signal of an individual event may contain some important features of the loads, the identification system would require much memory if all the WTCs are directly adopted as the features. As shown in Fig. 2, Parseval's theorem is therefore employed to extract the power spectrum of the WTCs as the features of the nonintrusive demand monitoring and load identification system. To equip the identification system with the ability to learn any arbitrary mapping of network input to desired output, the BP-ANN classification technique is utilized in this paper.

III. Proposed Methods

A. WT

Based on the characteristics of the bandpass filters, the WT has been proposed to investigate the transient phenomena of power signals from different scales of the WTCs. Particularly, transient phenomena with high-frequency components can be detected and located through adequate scales of the WTCs.

To overcome the extensive training requirement of applying STFT in NILM, Jean Morlet and Alex Grossman [21] proposed the concept of WT, i.e.,

$$\psi_{a,b}(t) = \frac{1}{\sqrt{a}}\psi\left(\frac{t-b}{a}\right), \quad a \in R^+,\ b \in R \tag{1}$$

where $\psi_{a,b}(t)$ is the daughter wavelet, $\psi(t)$ is the mother wavelet, a is the scaling factor, and b is the shift factor.

WT essentially uses scaling and shift factors to decompose the signal to be analyzed into a series of daughter wavelets. Therefore, it is suitable for analyzing transients [22]. WT can be classified into continuous WT (CWT), DWT, stationary WT, and wavelet packet transform. The CWT of a continuous-time signal $x(t)$ is defined as

$$w_{a,b} = \int_{-\infty}^{\infty} \psi_{a,b}(t)x(t)dt \tag{2}$$

where $x(t)$ is the original signal.

In order to determine the DWT, discretization of the scaling and shift factors is represented as follows:

$$\begin{aligned} a &= a_0^m \\ b &= nb_0\, a_0^m. \end{aligned} \tag{3}$$

Then, substituting (3) into (2), one will obtain

$$W_{m,n} = a_0^{-\frac{m}{2}} \sum_k x[k]\psi\left[a_0^{-m}k - nb_0\right], \quad a_0 > 1;\ b_0 \neq 0 \tag{4}$$

where m is a scaling number; n is a sampling time point, for $n = 1, 2, \ldots, N$; and N is the number of sampling points; m, $n \in Z$, Z is a set of integers, and k is an operating index.

Set

$$\begin{aligned} a_0 &= 2 \\ b_0 &= 1 \end{aligned} \tag{5}$$

then the following results:

$$W_{m,n} = 2^{-\frac{m}{2}} \sum_k x[k]\psi[2^{-m}k - n]. \tag{6}$$

The DWT essentially decomposes the original signal into detailed and approximate signals via high-pass, i.e., $h[n]$, and low-pass, i.e., $g[n]$, filters, respectively. The relationship between the high-pass and low-pass filters is as follows:

$$h[L-1-n] = (-1)^n\, g[n] \tag{7}$$

where L is the length of the filter.

As described above, due to various frequency components, the scales of the WTCs have been often employed to determine the occurrence of the load turn-on/off transient events by observing the high-frequency components. These high-frequency components are often resulted from the signals of the transient events. In this paper, Daubechies is used as the mother wavelet for the WT.

B. Power Spectrum of the WTCs

Parseval's theorem is often used to describe the unitary of any Fourier transform, particularly in physics and engineering. A Fourier series decomposes a periodic signal $f(t)$ into the sum of a set of harmonic oscillators and is derived as follows:

$$f(t) = \frac{1}{2}a_0 + \sum_{n=1}^{\infty} a_n \cos\left(\frac{n\pi t}{T}\right) + \sum_{n=1}^{\infty} b_n \sin\left(\frac{n\pi t}{T}\right) \quad (8)$$

$$\begin{pmatrix} a_0 = \frac{1}{T}\int_{-T}^{T} f(t)dt \\ a_n = \frac{1}{T}\int_{-T}^{T} f(t)\cos\left(\frac{n\pi t}{T}\right)dt \\ b_n = \frac{1}{T}\int_{-T}^{T} f(t)\sin\left(\frac{n\pi t}{T}\right)dt \end{pmatrix} \quad (9)$$

where T is the time of a cycle.

From the viewpoint of energy, (8) can be rewritten to be

$$\frac{1}{T}\int_{-T}^{T} f^2(t)dt = \frac{1}{2}a_0^2 + \sum_{n=1}^{\infty}\left(a_n^2 + b_n^2\right). \quad (10)$$

If the scaling function and the mother wavelet are an orthonormal basis set, the relationship between the power spectrum of the discrete signal $f[n]$ and each of the WTCs can be built by Parseval's theorem. The WT can separate the energy of a signal in time and frequency domains. As a result of the multiresolution analysis characteristics of the WT, an individual event turn-on/off transient signal can be represented by each scale of the WTCs, i.e.,

$$\text{WTC\_}f[n] = [|C_{J,k}\|d_{1,k}\|d_{2,k}|\ldots|d_{J,k}|] \quad (11)$$

where J is the number of the WT scale; and $C_{J,k}$ and $d_{j,k}$ are the coefficients of approximate and detailed versions of an individual event turn-on/off transient signal, respectively.

Consequently, through the DWT decomposition, the energy of the individual event turn-on/off transient signal is shown in (12). The first term on the right side of (12) denotes the average power of the approximated version of the decomposed signal, whereas the second term denotes the sum of the average power of the detailed version of the decomposed signal. Thus,

$$\frac{1}{N}\sum_{n=N}|f[n]|^2 = \frac{1}{N_J}\sum_{k}|C_{J,k}|^2 + \sum_{j=1}^{J}\left(\frac{1}{N_J}\sum_{k}|d_{j,k}|^2\right). \quad (12)$$

To filter the noise, $d_{1,k}$ coefficients are modified to be new ones $(d'_{1,k})$ by subtracting the standard deviation of the absolute wavelet coefficients from the absolute wavelet coefficients.

As stated in the preceding section, the second term in (12), the high-frequency components, will be employed to extract the features of load event in the NILM system, and it is denoted by P_{signal} in (13). The power spectrum of a turn-on/off event signal described by Parseval's theorem and the WTCs, the power spectrum of P_{signal} of each WTCs, can be obtained. The formula is shown in (14). Thus,

$$P_{\text{signal}} = \left(\frac{1}{N_J}\sum_{k}|d'_{j,k}|^2\right) = \frac{\|d_j\|^2}{N_j} \quad (13)$$

$$P_{\text{spectrum}} = (P_{\text{signal}})\frac{1}{2} = \left(\frac{\|d_j\|^2}{N_j}\right)^{\frac{1}{2}}. \quad (14)$$

Finally, as shown in (14), the energy of the event signal can be partitioned at different resolution levels in different ways depending on the sampling frequency. For example, the decomposition levels are adopted from 1 to 8 for the sampling frequency of 15 kHz to examine the coefficient of the detailed version at each resolution level for extracting the features of the event signal in the NILM system.

Furthermore, the following important properties in (14) for recognition features are listed below and have been confirmed via EMTP simulations and experiments.

1) The energy distribution remains unaffected by the turn-on/off time of load event.
2) The outline of the energy distribution remains similar to variations in the different current amplitudes of the same load type.
3) The low-level energy distribution will show obvious variations when the event signal contains high-frequency components.

For example, Fig. 3(a) shows a turn-on transient current waveform with three different turn-on times of occurrence for a 160-hp induction motor in an EMTP simulation. Employing (14) to analyze the three signals shows that the detailed energy distributions (scale 1 to scale 8) of the given signals are the same, as shown in Fig. 3(b). Furthermore, when the different current amplitude of the load event occurs, as shown in Fig. 4(a), the detailed versions of energy distributions (scale 1 to scale 8) are similar, as shown in Fig. 4(b).

Accordingly, the features of turn-on/off load signals can distinguish different load events using differences of the detailed version of energy distribution. As shown in Fig. 5, the six different loads labeled load 1 to load 6 are one 160-hp induction motor, one 123-hp induction motor driven by variable-voltage drives, one load bank supplied by a six-pulse thyristor rectifier from ac power, one 2.6-hp induction motor, one 4.7-hp induction motor, and one $R-L$ linear load with real and reactive powers equivalent to those of a 4.7-hp induction motor. The power spectrum in Fig. 5 expresses that the six different loads have different distributions of energy from scale 1 to scale 8. Consequently, in terms of the power spectrum in small scales (in high-frequency domain), different load events can be

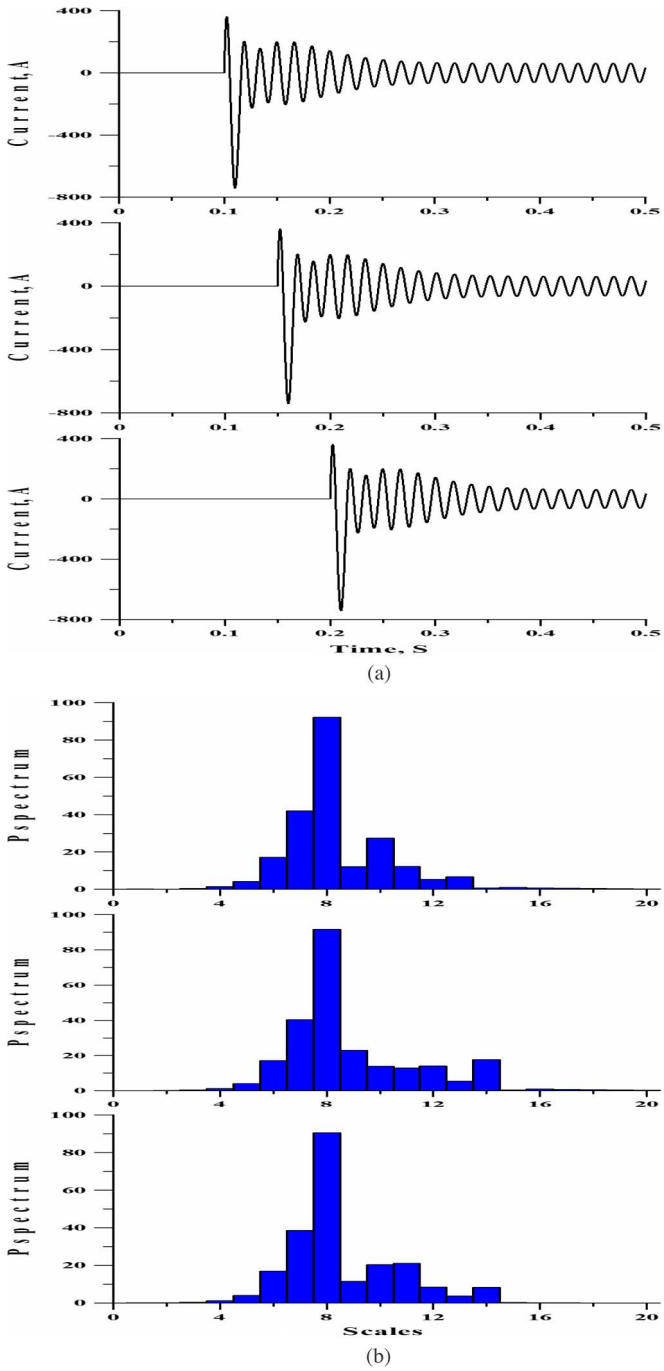

Fig. 3. Load event with different turn-on times of a 160-hp induction motor. (a) Different times of load current turn-on occurrence. (b) Power distribution diagrams.

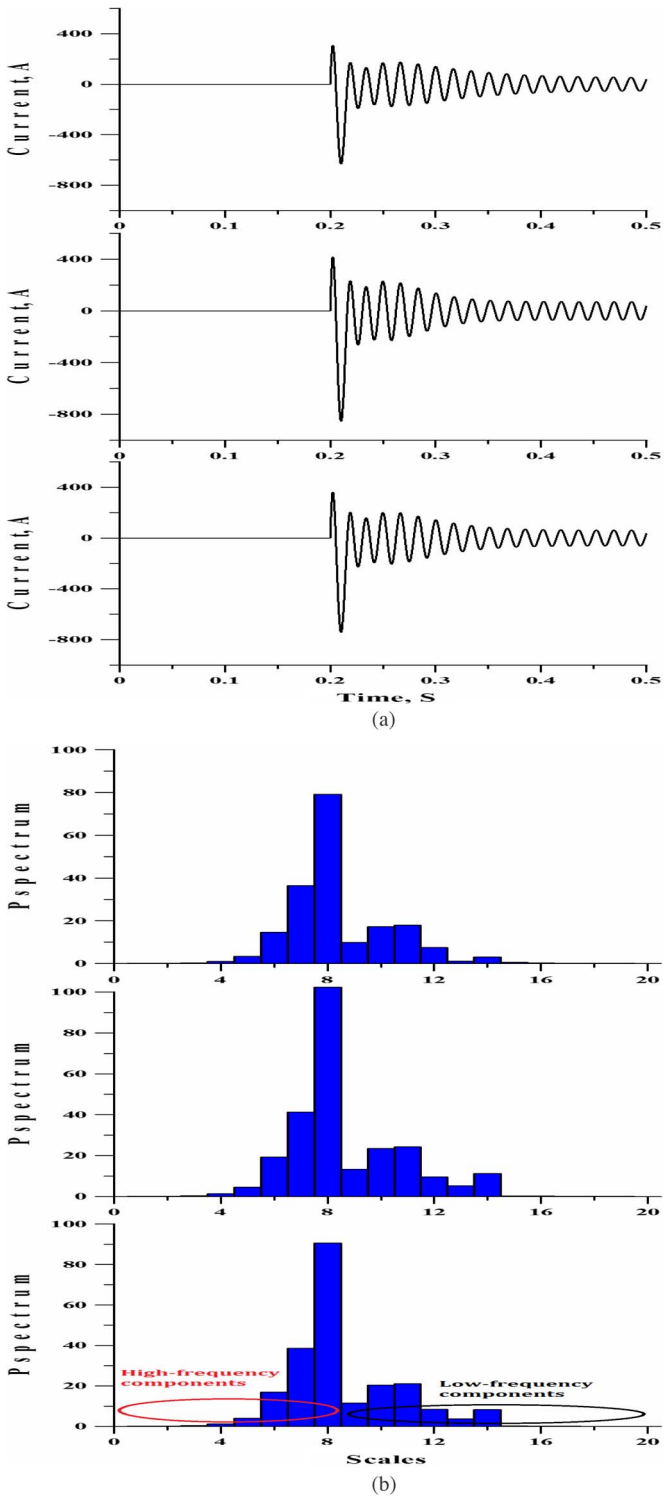

Fig. 4. Load event with different current amplitude magnitudes of a 160-hp induction motor. (a) Different amplitude magnitudes of load current turn-on occurrence. (b) Power distribution diagrams.

classified using particular energy spectra as the features in the NILM system.

C. ANNs

Pattern classifiers partition a multidimensional space into decision regions that indicate the class to which any input belongs [23].

1) Training Algorithms and Fitness Function: Overfitting is a typical problem that occurs during ANN training. Bayesian regularization [mean square error, (MSE)] typically provides better generalization performance than early stopping because it does not require a validation data set to be separated from the training data set. In other words, the input training data uses all training data sets. This advantage is particularly important when the available data set is small.

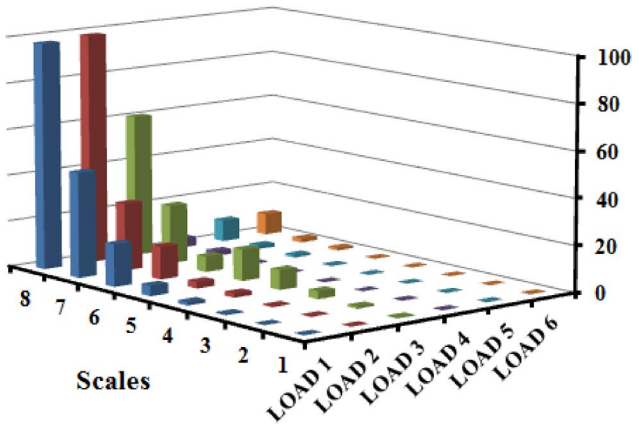

Fig. 5. Distributions of each scale for six different loads.

The typical fitness function used for training a feedforward NN is the mean sum of squares of network errors, which is also called MSE, which is the average squared error between network outputs and desired outputs, i.e.,

$$\text{MSE}(l) = \frac{1}{2}\sum_{j\in C}(t_j(l) - a_j(l))^2 \tag{15}$$

where $t_j(l)$ is the desired output for the lth iteration at node j, and $a_j(l)$ is the network output for the lth iteration at node j.

2) MFNN: Most BP-ANN applications utilize single- or multilayer perceptron networks by using gradient-descent training methods combined with learning via back propagation (BP). These multilayer perceptrons can be trained under supervision using analytical functions to activate network nodes ("neurons") and by applying a backward error propagation algorithm to update interconnecting weights and thresholds until a sufficient recognition capability is achieved. A trainable classifier uses the BP classifier for a multilayer feedforward NN (MFNN) in this study. "Classification" in this context is a mapping from a feature space to a set of class labels, which are the names of loads.

A supervised MFNN is generally divided into three layers: input, hidden, and output layers. These neurons are connected by links with weights that are selected to meet the desired relationship between input and output neurons. The MFNN in this study is utilized to identify loads in the NILM system. The input, output, and hidden layers of the BP-ANN are as follows.

1) *Input layer*: PS information, the energy spectra of a turn-on/off event signal, for an ESE serves as inputs.
2) *Output layer*: The number of output neurons is the same as the number of individual loads identified. Each binary bit serves as a load indicator for turn-on/off status.
3) *Hidden layer*: Only one hidden layer is used in this study. Some heuristics that can determine the number of neurons in a hidden layer have been developed [24]. The common number of neurons in a hidden layer is the sum of the number of neurons in an input layer and that in an output layer.

IV. Experimental Results

A. Study Environment

Experimental data sets were generated by preprocessing the data on the voltage and current waveforms of the total load. Each final sample consists of $(T \times 60 \times 256)$ samples obtained over a period of T. Each example of the power feature includes a voltage variation from -5% to $+5\%$ at 1% intervals, yielding 11 examples of power feature for each scenario and $N(N^2 - 3N + 4) \times 11$ raw data for $N + ((N-2)(N-1)+1)N$ scenarios, given that N loads can be only on or off at any given time in the system. The full input data set can form a matrix with a size of $(N(N^2 - 3N + 4) \times 11)$ by $(T \times 60 \times 256)$, which includes the training data set and the test data set. To confirm the inferential power of the NNs, the training data set and the test data set are created by two different scenarios, which are described as follows.

1) Scenario 1: The full raw data set is randomly divided into two halves, with equal size of data. One set of the data is for training and the other is for testing.
2) Scenario 2: The full raw data set is divided into two parts. One is with size of $N \times 11$ data and is used for training. The other is the test data set, having the size of $(N(N^2 - 3N + 3) \times 11)$ data.

An NN simulation program was designed using MATLAB. The program was run to identify loads on a personal computer equipped with a 3.3-GHz Intel Core i3-2120 central processing unit.

Each entry in the BP-ANN represents ten different trials, and each trial uses random initial weights. In each case, the network is trained until the MSE is less than 0.0001 or the number of iterations reaches 3000.

The proposed method is able to identify the loads instantly. The results of six different cases show the superiority of the proposed method.

B. Results

1) Case Study 1—EMTP Simulation: In case study 1, a simulated NILM system constructed by the EMTP software program monitors the voltage and current waveforms in a three-phase ESE powering representative loads in an industrial building. The NN algorithm in the NILM system identifies three loads on a 480-V common bus based upon the proposed power spectrum method (P_{spectra}), real and reactive power (PQ), and PQ together with turn-on transient energy (also called PQU_T) signatures [12]. These loads include a 160-hp induction motor, a 123-hp induction motor driven by line frequency variable-voltage drives, and a load bank supplied by a six-pulse thyristor rectifier for ac power.

Table I shows that values for the training accuracy of load identification in multiple operations are all 100% for features with the proposed, PQ, and PQU_T features. Furthermore, the test accuracy of load identification in multiple operations is near 100% in scenario 1 for all features. In terms of scenario 2, however, the identification rate of test is the highest for the proposed method, which uses P_{spectra} as the power signature.

TABLE I
RESULTS OF LOAD IDENTIFICATION IN CASE STUDY 1

Features	$P_{spectra}$	$P_{spectra}$	PQ	PQ	PQU_T	PQU_T
Scenario	1	2	1	2	1	2
Recognition Accuracy In Training (%)	100	100	100	100	100	100
Recognition Accuracy In Test (%)	100	96.67	100	0	99.09	6.97
Training Time (s)	0.46	0.42	1.08	0.92	0.83	0.69
Test Time (s)	0.007	0.007	0.007	0.007	0.007	0.007

TABLE II
RESULTS OF LOAD IDENTIFICATION IN CASE STUDY 2

Features	$P_{spectra}$	$P_{spectra}$	PQ	PQ	PQU_T	PQU_T
Scenario	1	2	1	2	1	2
Recognition Accuracy In Training (%)	100	100	71.82	100	100	100
Recognition Accuracy In Test (%)	97.12	88.48	59.39	0	93.94	44.65
Training Time (s)	0.54	0.48	17.90	0.69	0.95	0.43
Test Time (s)	0.009	0.008	0.008	0.007	0.008	0.007

Regarding the computation time, the time of training when the proposed features are used is shorter than those of PQ and PQU_T, regardless whether scenario 1 or scenario 2 is used.

2) Case Study 2—Experiment: The NILM system in case study 2 monitors the voltage and current waveforms in a single-phase ESE powering representative loads. The NN algorithm in the NILM system identifies three actual loads on a 110-V common bus with P_{spectra}, PQ, and PQU_T signatures. These loads include a 100-W television set, a 1200-W vacuum cleaner, and an 800-W hair dryer.

Table II shows that values for the test recognition accuracy of load identification in multiple operations of the proposed features are 97.12% in scenario 1, and it is also the highest among the others for the same scenario. In scenario 2, the proposed features can significantly enhance the test recognition accuracy of load recognition in multiple operations.

In this case, the property of these loads increases the difficulty of load identification for the NILM system. It is a problem concerning the real and reactive powers of these loads. The real and reactive powers of a 1200-W vacuum cleaner are much bigger than those of a 100-W television set. The television set is not easily to be recognized from the combination of the television set and the vacuum cleaner when voltage changes.

In terms of the computation time, the proposed features in general take less time for training when compared with others by using scenario 1 or scenario 2.

3) Case Study 3—EMTP Simulation for Different Loads With the Same Real and Reactive Powers: In case study 3, the NILM system monitors voltage and current waveforms in a three-phase ESE powering a collection of loads representative of the major load classes in a commercial building. The NN algorithm in the NILM system identifies three loads with P_{spectra}, PQ, and PQU_T signatures operating on a 220-V common bus. These loads include a 2.6-hp induction motor, a 4.7-hp induction motor, and an $R-L$ linear load with real and reactive powers equivalent to those of a 4.7-hp induction motor.

TABLE III
RESULTS OF LOAD IDENTIFICATION IN CASE STUDY 3

Features	$P_{spectra}$	$P_{spectra}$	PQ	PQ	PQU_T	PQU_T
Scenario	1	2	1	2	1	2
Recognition Accuracy In Training (%)	100	100	100	100	100	100
Recognition Accuracy In Test (%)	100	98.99	48.48	0	92.12	3.84
Training Time (s)	0.46	0.42	27.46	6.15	0.88	2.07
Test Time (s)	0.007	0.007	0.007	0.007	0.019	0.009

TABLE IV
RESULTS OF LOAD IDENTIFICATION IN CASE STUDY 4

Features	$P_{spectra}$	$P_{spectra}$	PQ	PQ	PQU_T	PQU_T
Scenario	1	2	1	2	1	2
Recognition Accuracy In Training (%)	100	100	85.91	100	98.94	100
Recognition Accuracy In Test (%)	96.82	86.16	66.36	0	90.93	4.65
Training Time (s)	0.54	0.49	17.90	6.93	0.95	4.28
Test Time (s)	0.009	0.008	0.008	0.007	0.008	0.007

Table III shows that the recognition accuracy of load identification in multiple operations of scenario 1 in training and test are 100% and 92.12%, respectively, for features with PQU_T. However, the test recognition accuracy of load identification in multiple operations of the same scenario is only 48.48% for features with PQ. Those loads cannot be identified by PQ features because the second and third loads are different loads with the same real and reactive powers, as are combinations of the first and second loads and combinations of the first and third loads. In other words, test recognition for those loads in multiple operations of scenario 1 is quite low when using only PQ features.

Moreover, the test recognition accuracy of load identification in multiple operations of scenarios 1 and 2 are 100% and 98.99%, respectively, for the proposed features.

4) Case Study 4—Experiment for Different Loads With Similar Real and Reactive Powers: In case study 4, the NILM system is used to monitor voltage and current waveforms in a single-phase ESE powering representative loads in the laboratory. The NN algorithm in the NILM system identifies three actual loads with P_{spectra}, PQ, and PQU_T signatures on a 110-V common bus. These loads include a 100-W television set, an 80-W desk lamp, and a 100-W electric fan.

Table IV shows that the training and test recognition accuracy of load identification in multiple operations of scenario 1 for PQU_T are 98.94% and 90.93%, respectively. However, the accuracy of training and test recognition of load identification in multiple operations of the same scenario are only 85.91% and 66.36%, respectively, for the PQ approach. The test recognition for those loads in multiple operations is also quite low when using only PQ features, regardless whether the scenario is scenario 1 or scenario 2. The reason for this is the same as that for the previous case study. In other words, the presence

TABLE V
RESULTS OF LOAD IDENTIFICATION IN CASE STUDY 5

Features	$P_{spectra}$	$P_{spectra}$	PQ	PQ	PQU_T	PQU_T
Scenario	1	2	1	2	1	2
Recognition Accuracy In Training (%)	100	100	100	33.33	100	100
Recognition Accuracy In Test (%)	100	0	39.47	0	98.42	0
Training Time (s)	0.49	0.43	1.94	7.13	7.41	3.63
Test Time (s)	0.008	0.008	0.010	0.009	0.011	0.013

TABLE VI
RESULTS OF LOAD IDENTIFICATION IN CASE STUDY 6

Features	$P_{spectra}$	$P_{spectra}$
Scenario	1	2
Recognition Accuracy In Training (%)	100	100
Recognition Accuracy In Test (%)	100	90.01
Training Time (s)	0.62	0.43
Test Time (s)	0.011	0.009

of different loads with the same real and reactive powers can be observed in two ways. First, test recognition in multiple operations is quite low when only using features of P and Q. Second, the turn-on transient energy for one of the features can improve load identification in scenario 1, particularly for different loads with similar real and reactive powers.

Furthermore, the test recognition accuracy of load identification in multiple operations of scenarios 1 and 2 are 96.82% and 86.16%, respectively, for the proposed features. In scenario 1, the test recognition accuracy of load identification in multiple operations for the proposed features is the highest among all the other features. In scenario 2, the proposed features can improve the training and test recognition accuracy and computation time of load identification in multiple operations compared with others.

5) Case Study 5—EMTP Simulation for Simultaneously Turn-On Loads With the Same Real and Reactive Powers: In case study 5, the NILM system monitors voltage and current waveforms in a three-phase ESE powering a collection of loads representative of the major load classes in a commercial building. The NN algorithm in the NILM system identifies three loads with P_{spectra}, PQ, and PQU_T signatures operating on a 220-V common bus. These loads are the same with those in case study 3.

Table V shows that values for the training and test recognition accuracy of load identification in multiple operations are all greater than 98.42% for PQU_T and P_{spectra} in scenario 1. However, the accuracy of training and test recognition of load identification in multiple operations are 100% and 39.47%, respectively, in the same scenario for the PQ approach. The test recognition for those loads in multiple operations is also quite low when using only PQ features in scenarios 1 and 2. The reason for this is the same as that for the previous case study.

In this case, since there is no information of loads with simultaneous turn-on in the training data for all features in scenario 2, the value of the test recognition accuracy of load identification in multiple operations is zero for all features, including the proposed features.

6) Case Study 6—EMTP Simulation for Turn-Off Loads With the Same Real and Reactive Powers: In case study 6, the NILM system monitors voltage and current waveforms in a three-phase ESE powering a collection of loads representative of the major load classes in a commercial building. The NN algorithm in the NILM system identifies three loads with P_{spectra}, PQ, and PQU_T signatures operating on a 220-V common bus. These loads are the same with those in case study 3.

Table VI shows that the training and test recognition accuracy of load identification in multiple operations are at least 90.01% for the proposed features in this case.

V. CONCLUSION

This paper has presented a novel NILM algorithm to improve the associated recognition accuracy. The proposed NILM algorithm applies Parseval's theorem to the WTCs of the energizing and deenergizing transient waveforms of individual or composite load operations to find out their energy spectra. The advantage of using the derived energy spectra as the PS is that it can capture the important features of the transient signals without requiring excessive memory space and training time. This is drastically different from other studies, employing all the WTCs to represent the transient phenomena. The energy spectra are then processed by the proposed BP-ANN for training and testing. To verify the validity of the proposed method, six different experimental and EMTP simulation case studies are investigated in this paper. Even the cases include some of the most challenging scenarios for a NILM system to identify, such as different loads with the same steady-state real and reactive powers, ratings of the loads cover wide spectrum, and simultaneously turned on/off load with the same real and reactive powers; the proposed method yields better recognition accuracy and shorter computation time, as compared with other existing methods such as PQ and PQU_T methods.

REFERENCES

[1] G. W. Hart, "Nonintrusive appliance load monitoring," *Proc. IEEE*, vol. 80, no. 12, pp. 1870–1891, Dec. 1992.
[2] C. Laughman, K. Lee, R. Cox, S. Shaw, S. Leeb, L. Norford, and P. Armstrong, "Power signature analysis," *IEEE Power Energy Mag.*, vol. 1, no. 2, pp. 56–63, Mar./Apr. 2003.
[3] M. Zeifman and K. Roth, "Nonintrusive appliance load monitoring: Review and outlook," *IEEE Trans. Consum. Electron.*, vol. 57, no. 1, pp. 76–84, Feb. 2011.
[4] J. Liang, S. K. K. Ng, G. Kendall, and J. W. M. Cheng, "Load signature study part I: Basic concept, structure, and methodology," *IEEE Trans. Power Del.*, vol. 25, no. 2, pp. 551–560, Apr. 2010.
[5] M. Akbar and Z. Khan, "Modified nonintrusive appliance load monitoring for nonlinear devices," in *Proc. INMIC*, 2007, pp. 1–5.
[6] H. H. Chang and H. T. Yang, "Applying a non-intrusive energy-management system to economic dispatch for a cogeneration system and power utility," *Appl. Energy*, vol. 86, no. 11, pp. 2335–2343, Nov. 2009.
[7] A. I. Albicki and A. Cole, "Data extraction for effective non-intrusive identification of residential power loads," in *Proc. IEEE Instrum. Meas. Technol. Conf.*, 1998, pp. 812–815.
[8] S. B. Leeb, S. R. Shaw, and J. L. Kirtley, "Transient event detection in spectral envelope estimates for nonintrusive load monitoring," *IEEE Trans. Power Del.*, vol. 10, no. 3, pp. 1200–1210, Jul. 1995.

[9] S. N. Patel, T. Robertson, J. A. Kientz, M. S. Reynolds, and G. D. Abowd, "At the flick of a switch: Detecting and classifying unique electrical events on the residential power line," in *Proc. Conf. Ubiquitous Comput.*, 2007, pp. 271–288.
[10] S. Gupta, M. S. Reynolds, and S. N. Patel, "ElectriSense: Single-point sensing using EMI for electrical event detection and classification in the home," in *Proc. Conf. Ubiquitous Comput.*, 2010, pp. 139–148.
[11] H. Y. Lam, G. S. K. Fung, and W. K. Lee, "A novel method to construct taxonomy of electrical appliances based on load signatures," *IEEE Trans. Consum. Electron.*, vol. 53, no. 2, pp. 653–660, May 2007.
[12] H. T. Yang, H. H. Chang, and C. L. Lin, "Load identification in neural networks for a non-intrusive monitoring of industrial electrical loads," *Comput. Supported Coop. Work Design IV, Lecture Notes Comput. Sci.*, vol. 5236, pp. 664–674, 2008.
[13] D. Srinivasan, W. S. Ng, and A. C. Liew, "Neural-network-based signature recognition for harmonic source identification," *IEEE Trans. Power Del.*, vol. 21, no. 1, pp. 398–405, Jan. 2006.
[14] H. H. Chang, L. S. Lin, N. Chen, and W. J. Lee, "Particle swarm optimization based non-intrusive demand monitoring and load identification in smart meters," in *Conf. Rec. IEEE IAS Annu. Meeting*, Las Vegas, NV, USA, Oct. 7–11, 2012, pp. 1–8.
[15] D. Lee, S. B. Leeb, L. K. Norford, P. R. Armstrong, J. Holloway, and S. R. Shaw, "Estimation of variable-speed-drive power consumption from harmonic content," *IEEE Trans. Energy Convers.*, vol. 20, no. 3, pp. 566–574, Sep. 2005.
[16] D. He, L. Du, Y. Yang, R. G. Harley, and T. G. Habetler, "Front-end electronic circuit topology analysis for model-driven classification and monitoring of appliance loads in smart buildings," *IEEE Trans. Smart Grid*, vol. 3, no. 4, pp. 2286–2293, Dec. 2012.
[17] L. Du, J. A. Restrepo, Y. Yang, R. G. Harley, and T. G. Habetler, "Nonintrusive, self-organizing, and probabilistic classification and identification of plug electric loads in smart buildings," *IEEE Trans. Smart Grid*, vol. 4, no. 3, pp. 1371–1380, Sep. 2013.
[18] H. H. Chang, K. L. Chen, Y. P. Tsai, and W. J. Lee, "A new measurement method for power signatures of non-intrusive demand monitoring and load identification," *IEEE Trans. Ind. Appl.*, vol. 48, no. 2, pp. 764–771, Mar./Apr. 2012.
[19] Z. L. Gaing, "Wavelet-based neural network for power disturbance recognition and classification," *IEEE Trans. Power Del.*, vol. 19, no. 4, pp. 1560–1568, Oct. 2004.
[20] M. S. Tsai and Y. H. Lin, "Modern development of an adaptive non-intrusive appliance load monitoring system in electricity energy conservation," *Energy*, vol. 96, pp. 55–73, Aug. 2012.
[21] Y. Meyer, *Wavelets: Algorithms and Applications*. Philadelphia, PA, USA: SIAM, 1993.
[22] D. C. Robertson, O. I. Camps, J. S. Mayer, and W. B. Gish, Sr., "Wavelets and electromagnetic power system transients," *IEEE Trans. Power Del.*, vol. 11, no. 2, pp. 1050–1058, Apr. 1996.
[23] L. K. Norford and S. B. Leeb, "Non-intrusive electrical load monitoring in commercial buildings based on steady-state and transient load-detection algorithms," *Energy Build.*, vol. 24, no. 1, pp. 51–64, 1996.
[24] Y. Y. Hong and B. Y. Chen, "Locating switched capacitor using wavelet transform and hybrid principal component analysis network," *IEEE Trans. Power Del.*, vol. 22, no. 2, pp. 1145–1152, Apr. 2007.

Hsueh-Hsien Chang (S'05–M'05) was born in Taoyuan, Taiwan, in 1966. He received the B.S. and M.S. degrees from National Taiwan University of Science and Technology, Taipei, Taiwan, in 1994 and 1996, respectively, and the Ph.D. degree from Chung Yuan Christian University, Jhongli, Taiwan, in 2009, all in electrical engineering.

From 1996 to 1998, he was a Project and System Engineer with ABB Ltd., Taipei. Since 2009, he has been an Assistant Professor with the Department of Electronic Engineering, JinWen University of Science and Technology, New Taipei, Taiwan. His current research interests are in neural networks and evolutionary computing applications in power and energy systems and power quality of power systems.

Dr. Chang is a member of the IEEE Power Engineering and IEEE Industry Applications Societies; The Institution of Engineering and Technology, U.K.; and the Taiwanese Association for Consumer Electronics. He was the recipient of the 2011 Prize Paper Award for the Power Systems Engineering Committee of the IEEE Industry Applications Society.

Kuo-Lung Lian (M'07) received the B.A.Sc. (Hons.), M.A.Sc., and Ph.D. degrees from the University of Toronto, Toronto, ON, Canada, in 2001, 2003, and 2007, respectively, all in electrical engineering.

From October 2007 to January 2009, he was a visiting Research Scientist with the Central Research Institute of Electric Power Industry, Japan. He is currently an Assistant Professor with the Department of Electrical Engineering, National Taiwan University of Science and Technology, Taipei, Taiwan.

Yi-Ching Su received the B.S. degree from National Taipei University of Technology, Taipei, Taiwan, in 2010, and the M.S. degree from National Taiwan University of Science and Technology, Taipei, in 2012, all in electrical engineering.

He is currently an Engineer with Chicony Electronics Company, Ltd., New Taipei, Taiwan. His research interests are energy management, power system engineering, and intelligence algorithms.

Wei-Jen Lee (S'85–M'85–SM'97–F'07) received the B.S. and M.S. degrees from National Taiwan University, Taipei, Taiwan, in 1978 and 1980, respectively, and the Ph.D. degree from The University of Texas at Arlington, Arlington, TX, USA, in 1985, all in electrical engineering.

Since 1985, he has been with The University of Texas at Arlington, where he is currently a Professor with the Department of Electrical Engineering and the Director of the Energy Systems Research Center. He has been involved in the revision of IEEE Standards 141, 339, 551, and 739 and DOT 3000 series development. He is the Project Manager of the IEEE/National Fire Protection Association Collaboration on Arc Flash Phenomena Research Project. He has been involved in research on utility deregulation, renewable energy, smart grid, microgrid, arc flash and electrical safety, load forecasting, power quality, distribution automation and demand-side management, power systems analysis, online real-time equipment diagnostic and prognostic systems, and microcomputer-based instruments for power system monitoring, measurement, control, and protection. He has served as the Primary Investigator (PI) or Co-PI of over 90 funded research projects. He has provided on-site training courses for power engineers in Panama, China, Taiwan, Korea, Saudi Arabia, Thailand, and Singapore. He has authored or coauthored more than 280 papers published in journals and conference proceedings. He has refereed numerous technical papers for the IEEE; The Institution of Engineering and Technology, U.K.; and other professional organizations.

Dr. Lee is the Vice Chair for Papers of the IEEE Industry Applications Society (IAS) Industrial and Commercial Power Systems Department. He is an Associate Editor for the IEEE IAS and the *International Journal of Power and Energy Systems*. He is a Registered Professional Engineer in the State of Texas.